Pis'ma v ZhETF, vol. 78, iss. 12, pp. 1279 – 1282 © 2003 December 25

Description of the CERN SPS data on the Landau–Pomeranchuk–Migdal effect for photon bremsstrahlung in quantum regime

B. G. Zakharov

L. D. Landau Institute for Theoretical Physics RAS, 117334 Moscow, Russia

Submitted 11 November 2003

We analyze within the light-cone path integral approach [4] the recent CERN SPS data [19] on the Landau–Pomeranchuk–Migdal effect for photon bremsstrahlung in quantum regime from 149, 207, and 287 GeV electrons. Calculations have been carried out treating accurately the Coulomb effects and including the inelastic processes. Comparison with experiment is performed accounting for multi-photon emission. Our results are in good agreement with the data.

PACS: 12.20.–m

1. Recently much attention has been attracted to suppression of radiation processes in media due to multiple scattering (the Landau-Pomeranchuk-Migdal (LPM) effect [1, 2]) both in QED [3 – 8]and QCD [9, 10, 4, 11] (for recent reviews, see [12, 13]). In QED new interest in the LPM effect stems from the first accurate measurements of the LPM suppression by the SLAC E-146 collaboration [14] for photon bremsstrahlung from 8 and 25 GeV electrons. A detailed analysis of these high statistics data requires more accurate calculations than that perform by Migdal [2] within the Fokker-Planck approximation. The interest in the LPM effect in QCD is connected with the study of parton energy loss in a hot QCD matter which can be produced in high energy AA-collisions at RHIC and LHC.

In [4] (see also [6, 15, 16]) we have developed a new approach to the LPM effect, which we call the light-cone path integral (LCPI) approach. This formalism is applicable for radiation processes in both QED and QCD. It is based on the path integral treatment of multiple scattering in the transverse coordinate representation developed in [17]. In [18] we have analyzed within the LCPI approach the SLAC data [14], and obtained excellent agreement with the data. For the data of Ref. [14] the photon fractional momentum is small $x \lesssim 0.06$ ($x = k/E$, k is the photon momentum, E is the beam energy), and the LPM suppression becomes visible for $x \lesssim 0.02$ where quantum recoil effects are unimportant. In the present paper we analyze within our approach new data on the LPM effect obtained in the CERN SPS experiment [19] for bremsstrahlung from 147, 207, and 287 GeV electrons. It is of clear interest because the SPS data allow one, for the first time, to compare theory with experiment in the kinematic region where quantum effects come into play. The kinematic range covered by the SPS data [19] is $0.01 \lesssim x < 1$, and the onset of the LPM effect occurs for $x \sim 0.1$ where quantum effects are important.

2. In the LCPI approach the cross section of an induced $a \to bc$ transition is expressed through the solution of a two-dimensional Schrödinger equation with an imaginary potential which is proportional to the cross section of interaction of $\bar{a}bc$ system with a medium constituent. For $e \to \gamma e$ transition the corresponding cross section is the dipole cross section for scattering of e^+e^- pair off an atom, $\sigma(\rho)$ (here ρ is the transverse distance between electron and positron), and the Hamiltonian reads

$$H = -\frac{1}{2\mu(x)}\frac{\partial^2}{\partial \boldsymbol{\rho}^2} + v(\boldsymbol{\rho}, z)\,, \tag{1}$$

$$v(\boldsymbol{\rho}, z) = -i\frac{n(z)\sigma(|\boldsymbol{\rho}|x)}{2}\,, \tag{2}$$

where the Schrödinger mass is $\mu(x) = Ex(1-x)$, and $n(z)$ is the number density of the target. The longitudinal coordinate z in (1), (2) plays the role of time. The probability distribution of one-photon emission, dP/dx, is given by [4]

$$\frac{dP}{dx} = 2\mathrm{Re}\int\limits_{-\infty}^{\infty} dz_1 \int\limits_{z_1}^{\infty} dz_2 \exp\left(-\frac{i\Delta z}{L_f}\right) \times$$
$$\times\, \hat{g}\left[\mathcal{K}(\boldsymbol{\rho}_2, z_2|\boldsymbol{\rho}_1, z_1) - \mathcal{K}_v(\boldsymbol{\rho}_2, z_2|\boldsymbol{\rho}_1, z_1)\right]\,|_{\boldsymbol{\rho}_1=\boldsymbol{\rho}_2=0}\,. \tag{3}$$

Here $\Delta z = z_2 - z_1$, $\mathcal{K}$ is the Green's function for the Hamiltonian (1), $\mathcal{K}_v$ is the vacuum Green's function for $v(\boldsymbol{\rho}, z) = 0$, $L_f = 2E(1-x)/m_e^2 x$, $\hat{g}$ is the vertex

operator accumulating spin effects (for its explicit form see [4]).

The dipole cross section can be written as $\sigma(\rho) = C(\rho)\rho^2$, where

$$C(\rho) = Z^2 C_{el}(\rho) + Z C_{in}(\rho). \tag{4}$$

Here the terms $\propto Z^2$ and $\propto Z$ correspond to elastic and inelastic interactions of e^+e^- pair with an atom. In the region $\rho \lesssim 1/m_e$, which is important for evaluation of the radiation rate (see below), $C_{el}(\rho)$ can be parametrized as

$$C_{el}(\rho) = 4\pi\alpha^2 \left[\log\left(\frac{2a_{el}}{\rho}\right) + \frac{(1-2\gamma)}{2} - f(Z\alpha)\right],$$
$$f(y) = y^2 \sum_{n=1}^{\infty} \frac{1}{n(n^2+y^2)}, \tag{5}$$

where $\alpha = 1/137$, $\gamma = 0.577$ is Euler's constant. The $C_{in}(\rho)$ can be written in a similar form (with a_{el} replaced by a_{in}) but without $f(Z\alpha)$. The parametrization of $C_{el}(\rho)$ corresponds to scattering of e^+e^- pair on the atomic potential $\phi(r) = (Ze/4\pi r)\exp(-r/a_{el})$. The first two terms in the square brackets on the right-hand side of (5) stem from the Born approximation, while the last one gives the Coulomb correction due to multiphoton exchanges. To account for the finite size of nucleus one should replace on the right-hand side of (5) ρ by R_A for $\rho \lesssim R_A$ (here R_A is the nucleus radius).

The parameters a_{el} and a_{in} can be adjusted by comparing the Bethe-Heitler cross section calculated via the dipole cross section [6]

$$\frac{d\sigma^{BH}}{dx} = \int d\boldsymbol{\rho}\, |\Psi_e^{e\gamma}(x,\boldsymbol{\rho})|^2 \sigma(\rho x) \tag{6}$$

(here $\Psi_e^{e\gamma}(x,\boldsymbol{\rho})$ is the light-cone wave function for the $e \to e\gamma$ transition) with that obtained within the standard approach using the Thomas–Fermi–Molier model [20]. This gives $a_{el} = 0.81 r_B Z^{-1/3}$ and $a_{in} = 5.3 r_B Z^{-2/3}$ [18].

Treating the potential (2) as a perturbation one can represent the spectrum (3) as

$$\frac{dP}{dx} = \frac{dP^{BH}}{dx} + \frac{dP^{abs}}{dx}, \tag{7}$$

where the first term

$$\frac{dP^{BH}}{dx} = nL\frac{d\sigma^{BH}}{dx} \tag{8}$$

is the Bethe–Heitler spectrum (L is the target thickness), and the second one is the absorptive correction responsible for LPM suppression [6]. We use this representation for the numerical calculations. The explicit form of the absorptive term and light-cone wave function entering (6) can be found in [6].

An important characteristic of the LPM effect is the in-medium coherence (formation) length of photon emission (we refer to it as $L_f^{\rm eff}$). In the sense of the representation (3) $L_f^{\rm eff}$ is simply the typical Δz. The $L_f^{\rm eff}$ is related to the dominating ρ-scale, $\rho_{\rm eff}$, via the diffusion relation $\rho_{\rm eff} \sim \sqrt{2L_f^{\rm eff}/\mu(x)}$. From it follows that for small LPM suppression (when $L_f^{\rm eff} \sim L_f$) $x\rho_{\rm eff} \sim 1/m_e$. For strong LPM effect $L_f^{\rm eff}$ and $\rho_{\rm eff}$ are determined by the interplay of the diffusion and absorption effects. From the diffusion relation and condition $nL_f^{\rm eff}\sigma(x\rho_{\rm eff})/2 \sim 1$, saying that absorption for the $e^+e^-\gamma$ system becomes strong at $\Delta z \sim L_f^{\rm eff}$, one obtains $x\rho_{\rm eff} \sim 1/m_e\sqrt{\eta}$, and $L_f^{\rm eff} \sim L_f/\eta$, where $\eta = 2[nE(1-x)C(1/m_e)/xm_e^4]^{1/2}$. Thus one sees that, as was said above, the spectrum is only sensitive to the behavior of $C(\rho)$ at $\rho \lesssim 1/m_e$.

Note that the Fokker-Planck approximation in momentum representation used in Migdal's analysis [2] corresponds to the replacement of $C(\rho)$ by $C(\rho_{\rm eff})$. Then the spectrum can be written via the oscillator Green's function. This approximation works well for strong LPM effect ($\eta \gg 1$) when the logarithm in (5) is much larger than unity. For the SPS conditions $\eta \lesssim 3$ and the logarithm in (5) is $\sim 4-5$. In such a regime neglecting the logarithmic dependence of $C(\rho)$ may give errors about 10–20%.

3. In [19] the experimenters used Ir target with thickness $L = 4.36\%\ X_0 = 0.128\,\text{mm}$, here X_0 is the radiation length, for Ir $X_0 \approx 2.94\,\text{mm}$ [20]. The spectra in the radiated energy were measured for $k > 2\,\text{GeV}$. Similarly to the SLAC data, the SPS spectra include multi-photon emission. Using the given above estimate for $L_f^{\rm eff}$ one can see that for the SPS conditions $L_f^{\rm eff}/L$ does not exceed $\sim 0.02 - 0.04$. Smallness of this quantity allows one to evaluate multi-photon emission in the probabilistic approach.

We write the spectrum in the radiated energy (we refer to it as dN/dx) as

$$\frac{dN(E,x)}{dx} = K(E,x)\frac{dP(E,x)}{dx}, \tag{9}$$

where $K(E,x)$ accounts for multi-photon effects. For the SPS kinematic domain N-photon emission with $N > 2$ can be neglected. Then in the probabilistic treatment of

the radiation of one and two photons one can obtain for $K(E,x)$ [1)]

$$K(E,x)=\exp\left[-\int\limits_x^1 dy\frac{dP(E,y)}{dy}\right]\left[1+\frac{1}{2}F(E,x,\delta)\right], \tag{10}$$

$$F(E,x,\delta)=\int\limits_\delta^{\delta/(1-x)} dy\frac{dP(E,y)}{dy}+$$

$$+\int\limits_\delta^1 dy\left[\frac{dP(E,y)}{dy}-\frac{dP(E(1-x),y)}{dy}\right]-$$

$$-\int\limits_\delta^{x-\delta} dx_1\left[\frac{dP(E,x_1)}{dx_1}+\frac{dP(E,x_2)}{dx_2}-\frac{1}{1-x_1}\times\right.$$

$$\left.\times\frac{dP(E,x_1)}{dx_1}\frac{dP(E(1-x_1),y_2)}{dy_2}\left(\frac{dP(E,x)}{dx}\right)^{-1}\right], \tag{11}$$

where $x_2=x-x_1$, $y_2=x_2/(1-x_1)$, $\delta=k_{\min}/E$. Although the expression (11) is infrared finite, we indicated explicitly dependence on the low energy cutoff $k_{\min}$. In our numerical calculations we take $k_{\min}=0.1\,\text{GeV}$. The results are practically insensitive to variation of this quantity. The inaccuracy of the above expression for the K-factor at the SPS conditions is $\lesssim 0.5\%$. This is clearly not worse than the accuracy of the probabilistic approach by itself.

4. In Figure we plotted the SPS data and our results obtained with (solid line) and without (dashed line) LPM suppression. In [19] the spectra in the radiated energy were presented in logarithmic bins (25 per decade). It corresponds to $rdN/d\log(k)$ with $r=2\tanh(\Delta/2)$, $\Delta=\log(10)/25$. This form is used in Figure. Besides the multi-photon emission we have taken into account photon absorption multiplying the theoretical spectra by $\langle K_{abs}\rangle\approx 1-L/2\lambda_{ph}$, where λ_{ph} is the photon attenuation length. This decreases the spectra by $\lesssim 1.5\%$. The theoretical spectra were multiplied by normalization coefficients, C_{norm}, that were adjusted at each energy to minimize χ^2. We obtained the values $C_{\text{norm}}=0.994\pm0.006$ ($\chi^2/N=1.08$), 0.982 ± 0.005 ($\chi^2/N=1.78$), and 0.944 ± 0.004 ($\chi^2/N=1.43$) for $E=287$, 207, and 149 GeV, respectively. One can see that the theoretical spectra (with LPM suppression) are in good agreement with the data.

5. To summarize, we have analyzed the recent SPS data [19] on the LPM effect for bremsstrahlung from 149, 207, and 287 GeV electrons. The calculations have been performed within the light-cone path integral formalism [4, 6]. We treat accurately the Coulomb effects and include the inelastic processes. The comparison with experiment is performed accounting for multi-photon emission and photon absorption. Our results are in good agreement with the data in the full studied kinematic range which includes the region of the onset of the LPM effect where the photon fractional momentum $x\sim 0.1$, and quantum recoil effects are important.

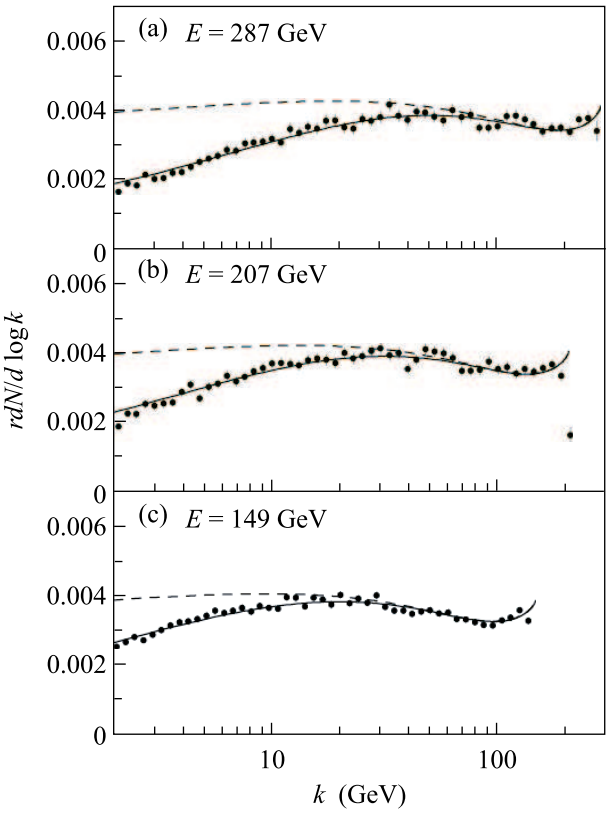

Comparison of the spectra in the radiated energy from the SPS experiment [19] with our calculations for bremsstrahlung from 287 (a), 207 (b), and 149 (c) GeV electrons on 4.36% X_0 Ir target. The solid line shows our results with LPM suppression. The dashed line shows the Bethe-Heitler spectrum. The multi-photon emission and photon absorption are taken into account. The Bethe-Heitler spectra are multiplied by the normalization coefficients obtained for the spectra with LPM suppression

I am grateful to Ulf-G. Meißner and J. Speth for the hospitality at FZJ, Jülich, where this work was completed. I would also like to thank U.I. Uggerhøj for sending the files of the experimental data and comments about some aspects of the SPS experiment. This work was partially supported by the grant DFG # 436RUS17/72/03.

[1)] This is a generalization to arbitrary x of the low-x K-factor derived in [18].

1. L. D. Landau and I. Ya. Pomeranchuk, Dokl. Akad. Nauk SSSR **92**, 535, 735 (1953).
2. A. B. Migdal, Phys. Rev. **103**, 1811 (1956).
3. R. Blankenbecler and S. D. Drell, Phys. Rev. **D53**, 6265 (1996).
4. B. G. Zakharov, JETP Lett. **63**, 952 (1996).
5. R. Baier, Yu. L. Dokshitzer, A. H. Mueller et al., Nucl. Phys. **B478** 577 (1996).
6. B. G. Zakharov, JETP Lett. **64**, 781 (1996).
7. R. Blankenbecler, Phys. Rev. **D55**, 190 (1997).
8. V. N. Baier and V. M. Katkov, Phys. Rev. **D57**, 3146 (1998).
9. R. Baier, Yu. L. Dokshitzer, S. Peigne, and D. Schiff, Phys. Lett. **B345**, 277 (1995).
10. R. Baier, Yu. L. Dokshitzer, A. H. Mueller et al., Nucl. Phys. **B483** 297 (1997).
11. B. G. Zakharov, JETP Lett. **65**, 615 (1997).
12. S. R. Klein, Rev. Mod. Phys. **71**, 1501 (1999).
13. R. Baier, D. Schiff, and B. G. Zakharov, Ann. Rev. Nucl. Part. Sci. **50**, 37 (2000).
14. P. L. Anthony, R. Becker-Szendy, P. E. Bosted et al., Phys. Rev. **D56**, 1373 (1997).
15. B. G. Zakharov, Phys. Atom. Nucl. **61**, 838 (1998).
16. B. G. Zakharov, JETP Lett. **70**, 176 (1999).
17. B. G. Zakharov, Sov. J. Nucl. Phys. **46**, 92 (1987).
18. B. G. Zakharov, Phys. Atom. Nucl. **62**, 1008 (1999).
19. H. D. Hansen, U. I. Uggerhøj , C. Biino et al., Phys. Rev. Lett. **91**, 014801 (2003).
20. Y.-S. Tsai, Rev. Mod. Phys. **46**, 815 (1974).